Dimensional scaling treatment of stability of simple diatomic molecules induced by superintense, high-frequency laser fields

Qi Wei,[1] Sabre Kais,[1,a)] and Dudley Herschbach[2]
[1]*Department of Chemistry and Birck Nanotechnology Center, Purdue University, West Lafayette, Indiana 47907, USA*
[2]*Department of Physics, Texas A&M University, College Station, Texas 77843, USA*

(Received 3 July 2008; accepted 23 October 2008; published online 3 December 2008)

We present results obtained using dimensional scaling with high-frequency Floquet theory to evaluate the stability of gas phase simple diatomic molecules in superintense laser fields. The large-D limit provides a simple model that captures the main physics of the problem, which imposes electron localization along the polarization direction of the laser field. This localization markedly reduces the ionization probability and can enhance chemical bonding when the laser strength becomes sufficiently strong. We find that energy and structure calculations at the large-dimensional limit ($D \to \infty$) for stabilities of H_2^+, H_2, and He_2 in superintense laser fields are much simpler than at $D=3$, yet yield similar results to those found from demanding *ab initio* calculations. We also use the large-D model to predict the stability of H_2^- and the field strength needed to bind the "extra" electron to the H_2 molecule. © *2008 American Institute of Physics*. [DOI: 10.1063/1.3027451]

I. INTRODUCTION

Atoms and molecules subjected to superintense radiation fields exhibit exotic properties, including above-threshold dissociation,[1] high-order harmonic generation,[2,3] charge resonance enhanced ionization,[4,5] and laser induced alignment.[6] Most striking is a paradoxical stabilization,[7] in which the ionization rate decreases as the radiation intensity increases.[8] In the high-frequency regime, the time-dependent Schroedinger equation for atoms and molecules in laser fields can be simplified to a time-independent form, termed high-frequency floquet theory (HFFT). By means of HFFT, gas phase atomic anions have been predicted to be stable in superintense high-frequency laser fields.[9–12] Similar stabilization has been predicted for some simple diatomic molecules.[13–17] As yet, however, such stabilization has not been demonstrated experimentally, except for atoms initially prepared in a high Rydberg state.[18]

According to HFFT, the stabilization in superstrong fields is accompanied by splitting of the electron distribution into distinct lobes, with locations governed by the quiver amplitude and polarization of the laser field. This localization markedly alters electron-nucleus interactions as well as reduces electron-electron repulsions and hence suppresses autoionization.[8,19] In molecules, it can also enhance chemical bonding.[14] Pronounced localization is likewise a characteristic feature of the large-D limit of dimensional scaling theory as applied to electronic structure.[20] We have indeed previously found that D-scaling, combined with HFFT, provides both an heuristic perspective and a useful technique to evaluate the stability of gas phase atomic anions subjected to superintense laser fields.[12] Calculations at large-D are much simpler than at $D=3$, yet gave similar results for the field strengths needed to bind an "extra" one or two electrons to H and He atoms.

In this paper, we apply the D-scaling method with HFFT to examine the stability in superintense laser fields of simple diatomics, H_2^+, H_2, H_2^-, and He_2, with respect to both ionization and bond dissociation. Our results, which require little computation, compare well with those obtained at $D=3$ from more arduous conventional calculations for H_2^+, H_2, and He_2. This encourages exploiting D-scaling with HFFT to treat larger molecules and to assess experimental prospects.

II. LASER-MOLECULE INTERACTION

We consider a high-frequency monochromatic electric field vector of the form

$$\mathbf{E}(t) = E_0(\mathbf{e}_1 \cos \omega t + \mathbf{e}_2 \tan \delta \sin \omega t), \tag{1}$$

with E_0 the amplitude, ω the frequency, $\mathbf{e}_j$ $(j=1,2)$ unit vectors orthogonal to each other and to the propagation direction of the light, $\delta=0$ corresponds to linear polarization, and $\delta = \pm \pi/4$ to circular polarization.[21] Except where indicated otherwise, we employ atomic units ($\hbar=e=m_e=1$); thus, distance is in bohrs (0.0529 nm), energy in hartrees (27.2 eV); 1 a.u. of field intensity $I=E_0^2$ is 3.51×10^{16} W/cm^2; of frequency ω is 4.13×10^{16} s^{-1}, equivalent to a wavelength of 45.9 nm. For a small molecule, miniscule compared with the wavelength of the light, the dipole approximation is well satisfied. Each electron within the molecule is then subject to the same laser field and undergoes quiver oscillations $\alpha(t)$ along a trajectory given by

$$\alpha(t) = \alpha_0(\mathbf{e}_1 \cos \omega t + \mathbf{e}_2 \tan \delta \sin \omega t), \tag{2}$$

where the quiver amplitude is $\alpha_0=E_0/\omega^2$. In the Kramers–Henneberger (KH) reference frame, translated by $\alpha(t)$ with respect to the laboratory frame, the electrons all remain

a)Electronic mail: kais@purdue.edu.

fixed; instead, the nuclei quiver along the $\alpha(t)$ trajectory. The Coulombic attraction between any electron and a nucleus with charge Z then takes the form $-Z/|\mathbf{r}_i+\alpha(t)|$. The HFFT approximation becomes valid when the field frequency ω is high compared with the typical frequency of electron motions within the molecule. The electrons then feel a time-averaged effective attractive potential, termed the "dressed potential," given by

$$V_0(\mathbf{r}_i,\alpha_0) = -\frac{Z}{2\pi}\int_0^{2\pi}\frac{d\Omega}{|\mathbf{r}_i+\alpha(\Omega/\omega)|}, \tag{3}$$

where $\Omega=\omega t$ and the time average extends over one period of the laser field.

For a homonuclear diatomic molecule with N-electrons and internuclear separation R, the Schroedinger equation in the KH frame is given by

$$\sum_{i=1}^{N}\left[\frac{1}{2}p_i^2+V_0\left(\mathbf{r}_i-\frac{\mathbf{R}}{2},\alpha_0\right)+V_0\left(\mathbf{r}_i+\frac{\mathbf{R}}{2},\alpha_0\right)+\sum_{j=1}^{i-1}\frac{1}{|\mathbf{r}_i-\mathbf{r}_j|}+\frac{Z^2}{R}\right]\Phi=\epsilon^{(N)}(\alpha_0,\mathbf{R})\Phi. \tag{4}$$

Since the Hamiltonian is Hermitian, the energy eigenvalues $\epsilon^{(N)}(\alpha_0)$ are real. The field parameters E_0 and ω appear only in the dressed potential and enter only via α_0, the quiver amplitude. Of prime interest are the bond energy and detachment energy,

$$\mathrm{BE}(N,\alpha_0,\mathbf{R}) = \epsilon^{(N)}(\alpha_0,\mathbf{R}\to\infty)-\epsilon^{(N)}(\alpha_0,\mathbf{R}) \tag{5}$$

$$\mathrm{DE}(N,\alpha_0,\mathbf{R}) = \epsilon^{(N-1)}(\alpha_0,\mathbf{R})-\epsilon^{(N)}(\alpha_0,\mathbf{R}). \tag{6}$$

As long as BE$>$0 and DE$>$0, the molecule remains intact and retains all of its electrons. This requires that $R>R^{\mathrm{crit}}$, the critical internuclear distance for which BE=0, and $\alpha_0>\alpha_0^{\mathrm{crit}}$, the critical quiver amplitude for which DE=0. The bond energy reaches maxima, denoted $\mathrm{BE}^{\mathrm{max}}=\mathrm{BE}(R^{\mathrm{max}})$, at somewhat larger distances, $R^{\mathrm{max}}>R^{\mathrm{crit}}$, that vary with α_0. For quiver amplitudes exceeding the critical value, the detachment energy has its maxima for the united atom (R=0) but typically remains positive for a substantial range of larger R.

III. RESULTS AT D=3

Previous applications of the HFFT to diatomic molecules, using D=3 methodology, pertain to linear polarization of the laser field and, for H_2^+ and H_2, to various values of the angle θ between the field direction and molecular axis.

For the H_2^+ case, Shertzer *et al.*[13] employed a Hamiltonian in the KH frame of the form

$$\left[\frac{\mathbf{\Pi}^2}{M}+\frac{\mathbf{P}^2}{2\mu}+\frac{1}{R}+V_0^-\left(\mathbf{r}-\frac{\mathbf{R}}{2};\alpha_0\right)+V_0^+\left(\mathbf{r}+\frac{\mathbf{R}}{2};\alpha_0\right)\right]u(\mathbf{R},\mathbf{r}) = Eu(\mathbf{R},\mathbf{r}), \tag{7}$$

where $\mathbf{p}$ and $\boldsymbol{\pi}$ are the electronic and nuclear momenta, $\mu=2mM/(m+2M)$ with m and M the electron and proton masses, and $V_0^{\pm}$ denote the dressed potential terms of our Eq. (3). The eigenvalues, determined by a finite element method, demonstrated that for the ground electronic state, as the field intensity is increased the molecular axis aligns more closely with the field direction (at θ=0° and 180°) and the maximum bond energy $\mathrm{BE}(R^{\mathrm{max}})$ increases steadily (from 2.6 eV at α_0=0 to 3.3 eV at α_0=5). As emphasized by Zuo and Bandrauk in a similar treatment of H_2^+, the increase in the bond energy with field strength is a generic effect.[14] This accords with Eq. (3), which makes it evident that the attractive potential energy is increased by the electric field.

For H_2, two approaches have been developed that enable HFFT calculations to be made using standard quantum chemistry programs. One, employed by Perez del Valle *et al.*, uses a multipole expansion of the dressed electron-nucleus interactions $V_0^{\pm}$ of Eq. (4) to determine equivalent point charge distributions.[15] The problem is then in effect reduced to electrons interacting with several quasinuclei having fractional charges. Applied to H_2, for $\alpha_0<2$, using just four quasinuclei gave good accuracy for the dressed potentials. The other method, developed by Nguyen and Nguyen-Dang, modifies molecular orbitals to incorporate dressed potentials in a fashion that permits use of the GAUSSIAN 94 package.[16] This method enabled calculations for much larger values of α_0, but required close analysis of methodology and use of relatively large basis sets. The chief focus was on the form of the charge distributions, particularly the dichotomous clustering of electron charge in the KH frame that occurs near the endpoints of the quiver oscillations of the nuclei. Neither of these studies discussed the enhancement of chemical bonding and stabilization against ionization of H_2, our prime interest.

For He_2 a thorough analysis of laser induced chemical bonding in the HFFT regime was made by Tomokazu and Someda.[17] They carried out extensive SCF-MO calculations

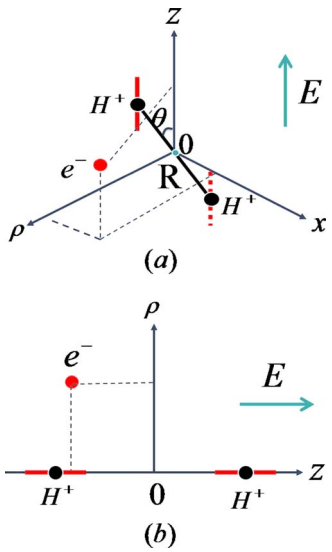

FIG. 1. (Color online) (a) The H_2^+ molecule ion as viewed in the Kramers–Henneberger frame: lines of charges [in (x–z) plane] of length $2\alpha_0$ arise from quiver amplitude of protons along the laser polarization direction (z-axis). Interaction of fixed electron with these lines of nuclear charge generates dressed potentials $V_0^{\pm}$ of Eq. (9). Angle θ is between the internuclear vector $\mathbf{R}$ and z-axis. (b) Special case with $\mathbf{R}$ along the polarization direction, so θ=0°.

TABLE I. Parameters for stability of H_2^+ in linearly polarized superintense laser fields.

α_0 (a.u.)			0.8		2.0	
	D	0	$\theta=0°$	$\theta=90°$	$\theta=0°$	$\theta=90°$
R^{crit} (a.u.)	3	1.1	1.3	1.6	1.8	2.8
	∞	0.62	0.83	0.95	1.3	1.6
R^{max} (a.u.)	3	2.0	2.2	2.7	3.3	4.2
	∞	1.2	1.6	1.7	2.9	3.0
BE^{max} (eV)	3	2.8	3.1	1.8	3.7	0.66
	∞	4.8	6.1	3.3	6.0	1.8
DE^{max} (eV)	3	54	⋯	⋯	⋯	⋯
	∞	54	36	36	22	22

and found that as the quiver amplitude grows, $BE(R^{max})$ increases dramatically (from zero at $\alpha_0=0-6$ eV at $\alpha_0=1$ and 13.9 eV at $\alpha_0=2$). From the study of the laser induced deformation of the molecular orbitals, they identify *sp* hybridization of the component atomic orbitals as the major source of the chemical bonding.

IV. EVALUATION AT LARGE-*D* LIMIT

The general procedure used in *D*-scaling[20] generalizes the Schroedinger equation (by endowing all vectors with *D* Cartesian components) and introduces *D*-scaled distance and energy units to remove the major, generic dimensional dependence. The large-*D* limit then yields a pseudoclassical structure, in which the electrons are localized in the *D*-scaled space, at positions determined by the minimum of an effective Hamiltonian function. This function contains no differential operators, but comprises merely a centrifugal term, derived from the kinetic energy, in addition to the usual Coulombic interactions among electrons and nuclei. As the scaling has removed most of the *D*-dependence, the energy at the $D\rightarrow\infty$ limit, found simply as the minimum of the effective Hamiltonian, typically offers a useful approximation to the $D=3$ energy.

This procedure provides a natural means to examine electron localization in a superintense laser field. Since in the KH frame the electrons are stationary, in that frame the HFFT becomes equivalent to the $D\rightarrow\infty$ limit, except that the electron-nuclear interactions are specified by the dressed potentials, with the nuclear charges distributed along the direction of polarization of the laser field. As we are concerned with linear polarization, it is convenient to use *D*-dimensional cylindrical coordinates (akin to $x=\rho\cos\phi$, $y=\rho\sin\phi$, and z, in $D=3$).[21] For a homonuclear diatomic molecule with *N* electrons, the corresponding HFFT version of the large-*D* limit effective Hamiltonian is then given by

$$\mathcal{H}=\frac{1}{2}\sum_{i=1}^{N}\frac{1}{\rho_i^2}+\sum_{i=1}^{N}V_0^{+}(\rho_i,z_i,\alpha_0)+\sum_{i=1}^{N}V_0^{-}(\rho_i,z_{i,},\alpha_0)+\sum_{i=1}^{N}\sum_{j=i+1}^{N}\frac{1}{\sqrt{\rho_i^2+\rho_j^2+(z_i-z_j)^2}}+\frac{\xi}{R}. \tag{8}$$

Here ξ/R is the repulsion energy between the two nuclei; it retains the same form in the KH frame since the nuclei are quivering synchronously. The scale parameter ξ must usually be assigned a value less than Z^2 to avoid overweighting the nuclear repulsion in the large-*D* limit.[22] For $Z=1$, we adopted $\xi=2/3$ to roughly match the large-*D* limit to $D=3$ results for H_2^+ and H_2 when there is no laser field; for $Z=2$, we used $\xi=4$. Comparison with $D=3$ results indicates that optimal values of ξ would vary with α_0, but for our purpose we preferred not to indulge that refinement. Again, the $V_0^{\pm}$ terms represent the dressed electron-nuclear interactions. As depicted in Fig. 1, we put the two nuclei in the *xz* plane with the origin midway between them and chose the laser polarization direction as the *z*-axis. The dressed potential terms then take the form

TABLE II. Parameters for stability of H_2 in linearly polarized superintense laser fields.

α_0 (a.u.)			1.0		2.0	
	D	0	$\theta=0°$	$\theta=90°$	$\theta=0°$	$\theta=90°$
R^{crit} (a.u.)	3	0.42	1.2	1.4	1.5	2.2
	∞	0.49	0.83	0.98	1.2	1.4
R^{max} (a.u.)	3	0.74	1.8	2.2	2.7	3.0
	∞	0.96	1.6	2.0	2.5	3.6
BE^{max} (eV)	3	4.2	5.1	2.0	5.1	0.83
	∞	6.0	5.8	2.8	5.2	1.6
DE^{max} (eV)	3	25	⋯	⋯	⋯	⋯
	∞	19	13	13	11	11

TABLE III. Parameters for stability of He_2 in linearly polarized superintense laser fields. For $\theta=90°$, the negative BE^{max} values given pertain to repulsive energies at R^{max}.

α_0 (a.u.)			1.0		2.0	
	D	0	$\theta=0°$	$\theta=90°$	$\theta=0°$	$\theta=90°$
R^{crit} (a.u.)	3	⋯	1.4	⋯	1.7	⋯
	∞	⋯	1.2	⋯	1.7	⋯
R^{max} (a.u.)	3	⋯	1.9	⋯	3.1	⋯
	∞	⋯	1.7	1.7	3.1	3.1
BE^{max} (eV)	3	0.0	6.0	⋯	14	⋯
	∞	0.0	12	−8.0	14	−5.0
DE^{max} (eV)	3	⋯	⋯	⋯	⋯	⋯
	∞	28	18	18	13	13

$$V_0^{\pm}(\rho,z,x;\theta;\alpha_0)=\frac{-Z}{2\pi}\int_0^{2\pi}\frac{d\phi}{\sqrt{\rho^2+\left(x\pm\frac{R}{2}\sin\theta\right)^2+\left(z\pm\frac{R}{2}\cos\theta+\alpha_0\sin\phi\right)^2}}. \tag{9}$$

Here ρ is the distance of the electron from the xz plane and θ is the angle between the internuclear axis **R** and the laser polarization direction. We will consider just two special cases, with **R** either parallel to ($\theta=0°$) or perpendicular to ($\theta=90°$) the laser polarization. We also treat only ground electronic states.

V. RESULTS AND DISCUSSION

Tables I–IV present bond dissociation energies and electron detachment energies and associated parameters, as obtained from our large-D limit version of HFFT. Where available, corresponding $D=3$ results are included. Figures 2–4 display the bond energy curves $BE(\alpha_0,R)$ for H_2^+, H_2, and He_2, respectively. Corresponding detachment energy curves $DE(\alpha_0,R)$ are not shown; the quantity of chief interest, DE^{max}, is included in the tables, and the α_0 dependence resembles that for atoms.[12]

For H_2^+, the bond strengths determined in the large-D limit are appreciably larger than those for $D=3$, but exhibit the same trends with R, θ, and α_0. In particular, as α_0 increases, the bond dissociation energy BE^{max} increases for $\theta=0°$ but decreases for $\theta=90°$. However, as α_0 increases the detachment energy for removal of the electron, DE^{max}, decreases and is the same for $\theta=0°$ and $\theta=90°$. As seen in the right hand panels of Fig. 2, when scaled to BE^{max} and R^{max}, the shape of the $BE(R)$ curves for $D\to\infty$ is similar to those for $D=3$ near R^{max}, but approaches the dissociation asymptote more slowly at large R, especially for $\theta=90°$.

For H_2, the large-D limit gives results generally like those for $D=3$ and displays the same trends as seen for H_2^+. Thus, again the bond strength, BE^{max}, is substantially higher for $\theta=0°$ than for $\theta=90°$, whereas the detachment energy does not change as θ is varied.

For He_2, the large-D results likewise resemble the much less extensive results available for $D=3$. For $\theta=0°$, the laser induced chemical bond strength for He_2 increases strongly with the quiver amplitude, much more strongly than for H_2; as evident from Eq. (9), this is a direct consequence of the increased number and magnitude of the dressed electron-nucleus interactions. The scaled $BE(R)$ curves for the large-D limit are in this case very close to those for $D=3$. For $\theta=90°$, only the large-D results are available at present, but indicate that increase in α_0 does not induce chemical bonding but rather augments repulsive interaction. The differences in BE between $\theta=0°$ and 90° seen for H_2^+ and H_2 thus for He_2 become much more pronounced. Again, DE^{max} does not depend on θ and decreases as α_0 is increased.

Figure 5 summarizes the trends in bond energy. From the perspective of the KH frame, a heuristic explanation for the major difference between $\theta=0°$ and $\theta=90°$ is evident from Fig. 1. For linear polarization, the quiver oscillation spreads the charge of each nucleus over $2\alpha_0$ but concentrates it near the endpoints of the oscillation. The consequent enhance-

TABLE IV. Parameters for stability of H_2^- in in linearly polarized superintense laser fields for $\theta=0°$ at large-D limit.

α_0 (a.u.)	1.5	2.0	2.5	4	6	8	10
R^{crit} (a.u.)	2.0	2.1	2.2	1.9	2.0	2.4	2.7
R^{max} (a.u.)	2.3	3.0	3.6	6.0	9.3	13	16
BE^{max} (eV)	5.7	5.9	6.0	5.1	4.4	3.9	3.4
DE^{max} (eV)	0.67	1.3	1.7	2.0	2.0	1.9	1.8

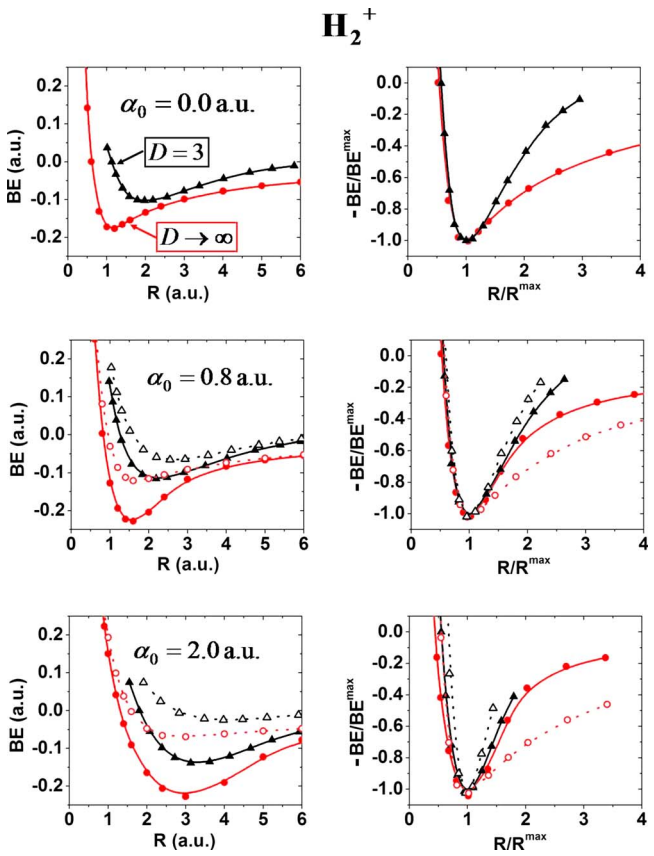

FIG. 2. (Color online) Bond energy for ground electronic state of H_2^+ vs bond length R for HFFT regime of linearly polarized superintense laser field. Results are shown for $D=3$ (triangles, from Ref. 13) and for large-D limit (circles) for field-free case ($\alpha_0=0$) and for fields with quiver amplitudes of $\alpha_0=0.8$ and 2.0 a.u. Laser polarization is parallel ($\theta=0°$, solid curves) or perpendicular to the internuclear axis ($\theta=90°$, dashed curves). Zero of energy refers to dissociation asymptote to form $H+H^+$. Panels at right show corresponding scaled curves, BE/BE^{max} vs R/R^{max}.

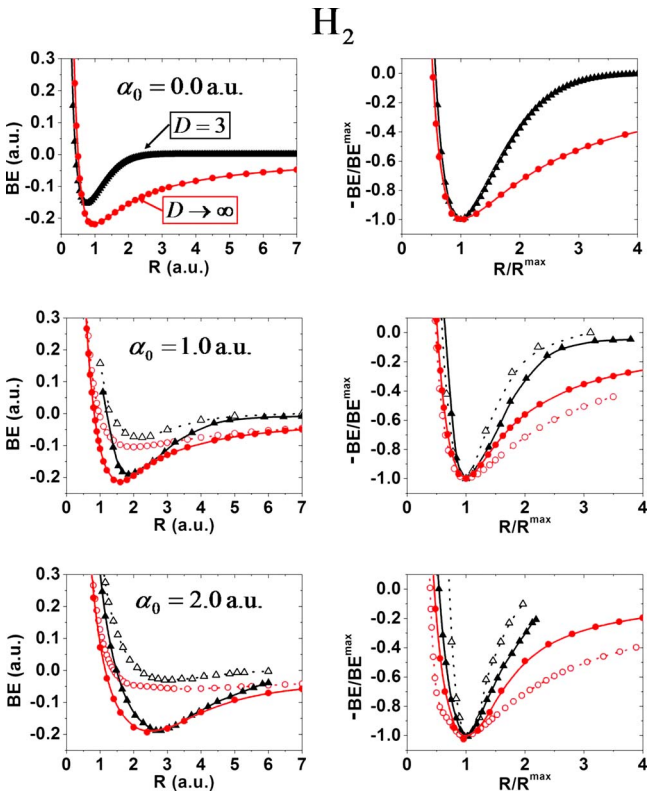

FIG. 3. (Color online) Bond energy for ground electronic state of H_2 molecule subject to superintense laser field. Format as in Fig. 2, except that dissociation asymptote pertains to H+H.

ment of electron density near those endpoints, termed "dichotomy," is a characteristic feature of the HFFT regime.[23] For a homonuclear diatomic molecule, the effect roughly amounts to splitting the positive charges among four quasinuclei, each with charge $Z/2$ and arrayed in pairs, the quasinuclei within each pair separated by $2\alpha_0$ and each pair aligned with the laser polarization, as indicated by the "lines of charge" in Fig. 1. When the internuclear axis R between midpoints of the quasipairs is parallel to the laser polarization ($\theta=0°$), the dichotomy effect fosters an increase in electron density between the nuclei and thus strengthens chemical bonding.[14] When R is perpendicular to the polarization ($\theta=90°$), the dichotomy draws electron density away from the region between the nuclei and weakens bonding.

For H_2^-, our large-D limit results (obtained only for $\theta=0°$) are presented in Figs. 6 and 7 and Table IV; no $D=3$ results are available for comparison. In our previous work on atomic anions,[12] we found that for H^- in the HFFT regime the critical quiver amplitude is $\alpha_0^{crit}=3$ a.u. Thus, unless $\alpha_0>3$ a.u., an electron cannot attach to a hydrogen atom in a laser field. An electron can attach to a hydrogen molecule even when $\alpha_0<3$ a.u. but then it can remain attached (i.e., $DE>0$) only for a finite range of the internuclear distance R,

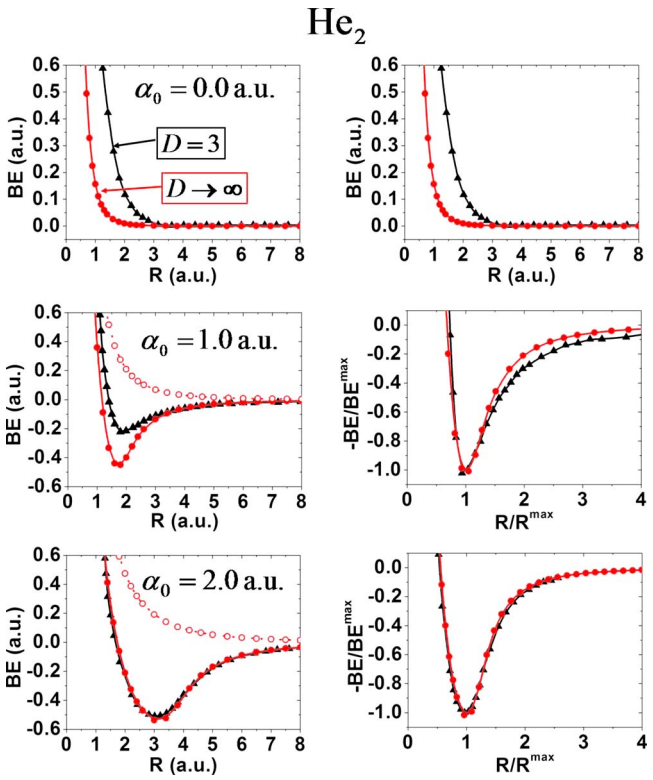

FIG. 4. (Color online) Bond energy for He_2 dimer subject to superintense laser field. Format as in Fig. 2, except that dissociation asymptote pertains to He+He.

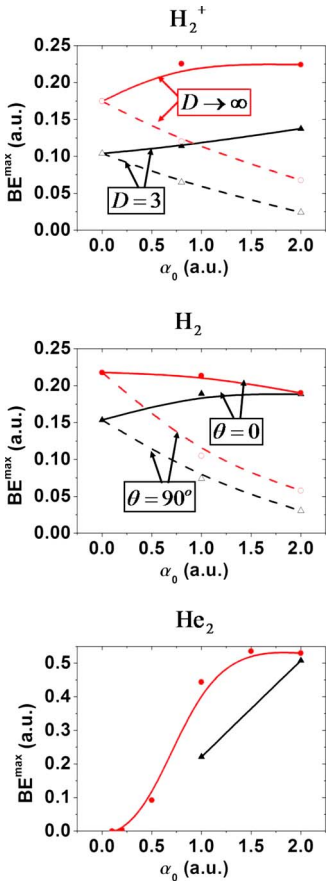

FIG. 5. (Color online) Variation in bond energy, BE^{max} (in a.u.), with quiver amplitude α_0 for H_2^+, H_2, and He_2. Results for $D=3$ indicated by triangles; for large-D limit by circles; full symbols and curves pertain to $\theta=0°$, open symbols and dashed curves to $\theta=90°$. For H_2^+ and H_2, as the quiver increases from $\alpha_0=0$ to 2, the bond energy increases for $\theta=0°$ but decreases for $\theta=90°$. For He_2, at $\alpha_0=0$ the bond energy is zero but for $\theta=0°$ it increases steeply with α_0; however, for $\theta=90°$ the bond energy becomes strongly negative with increasing α_0, as seen in Fig. 4. The markedly different variation in bond energy with θ found for H_2^+ and H_2 thus becomes much more pronounced for He_2.

as seen in Fig. 6. For this range, as α_0 increases BE^{max} remains nearly constant whereas DE^{max} increases strongly. When $\alpha_0>3$ a.u., since H^- is then always stable, the H_2^- anion remains stable for any $R>R^{crit}$, as seen in Fig. 7. In this range, as α_0 increases BE^{max} decreases whereas DE^{max} remains nearly constant.

This contrast between electron attachment for quiver amplitudes below and above 3 a.u. is further illustrated in Fig. 8. The fixed electron locations ("Lewis structure") attained at the $D\to\infty$ limit are shown for $\alpha_0=2.5$ (at left) and $\alpha_0=8$ (at right) and a wide range of internuclear distances. In both cases, the electron distribution broadens as either the quiver amplitude or R increases. The ρ-coordinates of the outermost electrons change only modestly with changes in R, whereas ρ for the central electron varies markedly. Likewise, the z-coordinates of the outermost electrons remain close to $\pm(\alpha_0+R/2)$ except when the central electron shifts away from $z=0$, thus disrupting the symmetrical configuration. Again, these features track directly changes in the form of the dressed potentials of Eq. (9), influenced by the dichotomy effect.

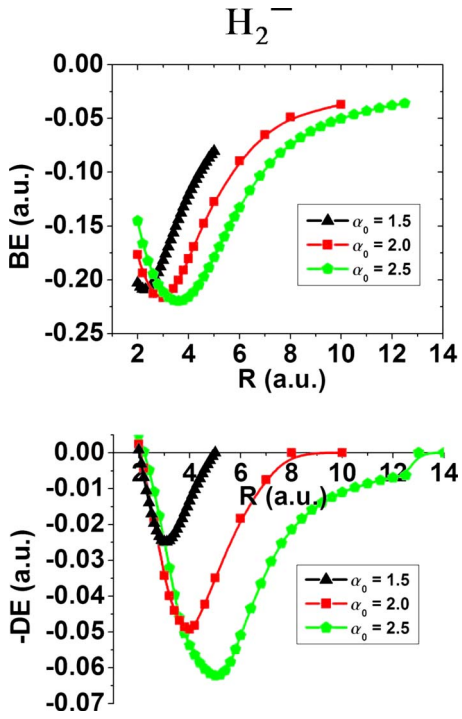

FIG. 6. (Color online) Bond energy and detachment energy for H_2^- molecule ion subject to superintense laser field in HFFT regime, as evaluated from large-D limit. For linearly polarized field with $\theta=0°$, with quiver amplitudes of $\alpha_0=1.5$, 2.0, and 2.5 a.u., values below $\alpha_0^{crit}=3.0$ a.u. for H^-.

VI. CONCLUSIONS

In view of the computational simplicity of the large-D limit version of HFFT, it is gratifying that it gives modest accuracy when compared with conventional $D=3$ methods.

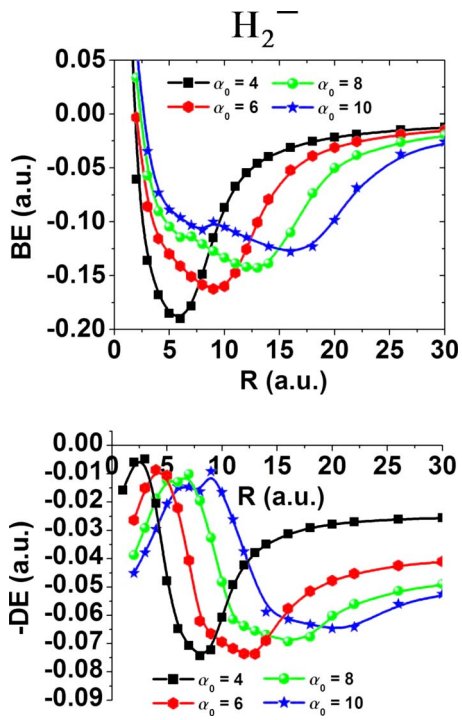

FIG. 7. (Color online) Bond energy and detachment energy for H_2^-; format as in Fig. 6 but for quiver amplitudes $\alpha_0=4$, 6, 8, and 10 a.u., exceeding the critical value of 3 a.u. for H^-.

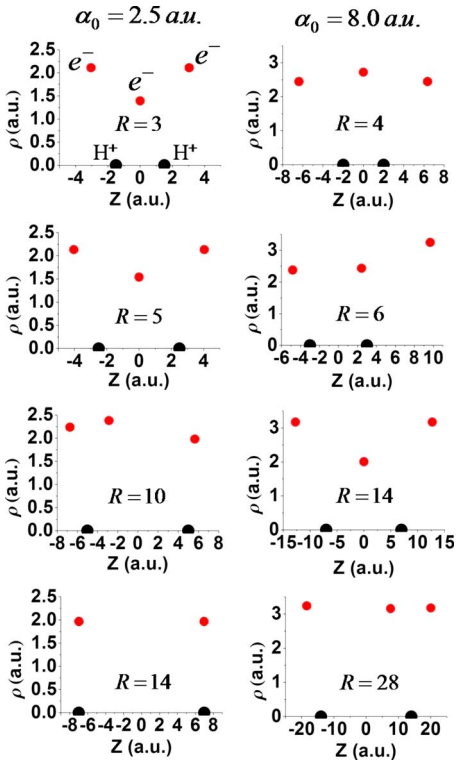

FIG. 8. (Color online) Variation in electronic structures (Lewis structures) at large-D limit for H_2^- in linearly polarized ($\theta=0°$) superintense laser fields for $\alpha_0=2.5$ (panels at left) and 8 a.u. (panels at right) and various bond lengths R. Positions of the protons (black dots) are fixed along the z-axis) and the electrons (red dots) are in the (ρ-z) plane. As seen in Fig. 5, when $\alpha_0<3$, the extra electron remains attached only for a finite range of R (thus is missing in the $R=14$ panel at left). In contrast, when $\alpha_0>3$, as seen in Fig. 6, all three electrons remain attached even as R grows very large (panels at right).

At present, this appears adequate to assess prospects for experimental tests of the predicted stabilization, both with respect to electron detachment and enhancement of chemical bonding. The HFFT approximation itself is subject to validity criteria[24] that in practice likely introduce uncertainties larger than disparities between the large-D and $D=3$ results.

The HFFT criteria impose upper and lower bounds on ω, the oscillation frequency of the radiation field,

$$137/\alpha_0 \gg \omega \gg [\epsilon^{(N)}(\alpha_0,R)]. \tag{10}$$

The upper bound is required to ensure that both the dipole approximation holds (radiation wavelength large compared with $2\alpha_0$) and a nonrelativistic treatment suffices (maximum quiver speed much lower than speed of light). The lower bound requires that the field must oscillate much faster than electron motion within the molecule. This is specified by an average excitation energy in the field,[13] usually estimated by the energy eigenvalue that appears on the right hand side of Eq. (4). For small α_0, this is typically comparable to the field-free ionization energy, but for large α_0 is often much smaller.[16,17]

Here we are concerned chiefly with small α_0, and the lower bound in Eq. (10) is of the order of 1 a.u. Even to barely match this bound with $\omega=1$ a.u. would require a laser near the frontier of current technology, delivering photons with energy of ~27 eV and wavelength of ~50 nm; for $\alpha_0=1$, the beam flux needed, $I=\alpha_0^2\omega^4$, would be $I\sim 1$ a.u.$=3.5\times10^{16}$ W/cm^2. Harmonic generation techniques are being pursued to develop such short-wavelength lasers.[25] Although the lower bound can be reduced by employing larger quiver amplitudes, for a given that would also push down the upper bound and increase the required intensity. Thus, experimentally, at present both bounds of Eq. (10) can rarely be fulfilled, certainly not with "much larger" inequalities. From this perspective, the HFFT has the status of an idealized theoretical limit that can offer only a rough guide to design and analysis of experiments.

Illustrative of the utility of our simple large-D version of HFFT as a qualitative guide is the evidence (Figs. 4 and 5) for the strong variation in laser induced bonding with the angle θ between the internuclear axis and the polarization of the laser field. This seems likely to be a robust property observable even if the constraints of Eq. (10) are not fulfilled. Yasuike and Someda have advocated a molecular beam experiment, colliding pairs of He atoms in an intense laser field.[17] The angular distribution of scattering would reveal the presence of an attractive intermolecular potential well and its dependence on laser polarization and the quiver amplitude. Such experiments, exploiting strong laser fields to steer electron paths within collision partners, would open a new route to exploring chemical stereodynamics.

ACKNOWLEDGMENTS

We are grateful for support of this work by a Department of Energy BES grant (DE-FG2-01ER15197). We thank also Marlan Scully for the opportunity to attend his Casper workshop, supported by the Institute for Quantum Studies at Texas A&M, where we recognized the virtues of treating the HFFT in the large-D limit.

[1] P. Agostini, F. Fabre, G. Mainfray, G. Petite, and N. K. Rahman, Phys. Rev. Lett. **42**, 1127 (1979).
[2] M. Y. Ivanov, P. B. Corkum, and P. Dietrich, Laser Phys. **3**, 375 (1993).
[3] T. Zuo, S. Chelkowski, and A. D. Bandrauk, Phys. Rev. A **49**, 3943 (1994).
[4] T. Seideman, M. Y. Ivanov, and P. B. Corkum, Phys. Rev. Lett. **75**, 2819 (1995).
[5] T. Zuo, and A. D. Bandrauk, Phys. Rev. A **52**, R2511 (1995).
[6] B. Friedrich, and D. R. Herschbach, Phys. Rev. Lett. **74**, 4623 (1995); V. Kumarappan, S. S. Viftrup, L. Holmegaard, C. Z. Bisgaard, and H. Stapelfeldt, Phys. Scr. **76**, C63 (2007).
[7] Mihai Gavrila, J. Phys. B **35**, R147 (2002).
[8] J. H. Eberly and K. C. Kulander, Science **262**, 1229 (1993).
[9] M. Gavrila, in *Atoms in Super Intense Laser Fields*, edited by M. Gavrila (Academic, New York, 1992), p. 435.
[10] E. van Duijn, M. Gavrila, and H. G. Muller, Phys. Rev. Lett. **77**, 3759 (1996).
[11] Q. Wei, S. Kais, and N. Moiseyev, J. Chem. Phys. **124**, 201108 (2006).
[12] Q. Wei, S. Kais, and D. Herschbach, J. Chem. Phys. **127**, 094301 (2007).
[13] J. Shertzer, A. Chandler, and M. Gavrila, Phys. Rev. Lett. **73**, 2039 (1994).
[14] T. Zuo and A. D. Bandrauk, Phys. Rev. A **51**, R26 (1995).
[15] C. Perez del Valle, R. Lefebvre, and O. Atabrek, J. Phys. B **30**, 5137 (1997); Int. J. Quantum Chem. **70**, 199 (1998).
[16] N. A. Nguyen, and T. T. Nguyen Dang, J. Chem. Phys. **112**, 1229 (2000).
[17] T. Yasuike and K. Someda, J. Phys. B **37**, 3149 (2004).
[18] N. J. van Druten, R. C. Constantinescu, J. M. Schins, H. Nieuwenhuize, and H. G. Muller, Phys. Rev. A **55**, 622 (1997); M. P. de Boer, J. H. Hoogenraad, R. B. Vrijen, R. C. Constantinescu, L. D. Noordam, and H. G. Muller, *ibid.* **50**, 4085 (1994).
[19] N. Moiseyev and L. S. Cederbaum, J. Phys. B **32**, L279 (1999).

[20] D. R. Herschbach, J. Avery, and O. Goscinski, *Dimensional Scaling in Chemical Physics* (Kluwer, Dordrecht, 1993).
[21] D. D. Frantz, and D. R. Herschbach, Chem. Phys. **126**, 59 (1988).
[22] C. A. Traynor and D. Z. Goodson, J. Phys. Chem. **97**, 2466 (1993).
[23] M. Pont, N. R. Walet, M. Gavrila, and C. W. McCurdy, Phys. Rev. Lett. **61**, 939 (1988).
[24] E. van Duijn and H. G. Muller, Phys. Rev. A **56**, 2182 (1997).
[25] K. Midorikawa, Opt. Lett. **27**, 3170 (2002).